Metabolism drives demography in an experimental field test

Lukas Schuster[a,1,2], Hayley Cameron[a,1], Craig R. White[a], and Dustin J. Marshall[a]

[a]Centre for Geometric Biology, School of Biological Sciences, Monash University, Melbourne, VIC 3800, Australia

Edited by Nils Chr. Stenseth, Universitetet i Oslo, Oslo, Norway, and approved July 19, 2021 (received for review March 14, 2021)

Metabolism should drive demography by determining the rates of both biological work and resource demand. Long-standing "rules" for how metabolism should covary with demography permeate biology, from predicting the impacts of climate change to managing fisheries. Evidence for these rules is almost exclusively indirect and in the form of among-species comparisons, while direct evidence is exceptionally rare. In a manipulative field experiment on a sessile marine invertebrate, we created experimental populations that varied in population size (density) and metabolic rate, but not body size. We then tested key theoretical predictions regarding relationships between metabolism and demography by parameterizing population models with lifetime performance data from our field experiment. We found that populations with higher metabolisms had greater intrinsic rates of increase and lower carrying capacities, in qualitative accordance with classic theory. We also found important departures from theory—in particular, carrying capacity declined less steeply than predicted, such that energy use at equilibrium increased with metabolic rate, violating the long-standing axiom of energy equivalence. Theory holds that energy equivalence emerges because resource supply is assumed to be independent of metabolic rate. We find this assumption to be violated under real-world conditions, with potentially far-reaching consequences for the management of biological systems.

competition | Damuth's law | energy equivalence | increased intake hypothesis | metabolic theory

Metabolism is thought to drive demography by setting the rate of biological work and resource consumption. For instance, theory predicts that metabolic rate should determine a population's carrying capacity by setting per capita resource demands (1–5). The idea that carrying capacity—the density at which a population stops growing—is linked to metabolism has intuitive appeal. Because higher metabolic rates are associated with higher resource demands, a population's carrying capacity (in terms of number of individuals) should be inversely proportional to metabolic rate (MR). In other words, carrying capacity (K) should scale at an exponent of MR^{-1} (1, 3, 4). Similarly, because metabolism powers the biological work of production and time to first reproduction, organisms with higher mass-specific metabolic rates should be able to replicate themselves faster. Accordingly, theory predicts that the rate at which populations grow should be proportional to mass-specific metabolic rate—that is, the intrinsic rate of increase (r) of populations should scale at an exponent of MR^{1} (6, 7). The idea that metabolic rate mechanistically determines population processes is well accepted (5), providing an explanation for biogeographical patterns and informing projections of the impacts of global change (8). Yet empirical support for relationships between metabolic rate and demography is largely indirect, mostly in the form of among-species comparisons of organisms that also differ in body size and temperature range. In contrast, these relationships have rarely been tested directly within species.

Among species, metabolic rate strongly covaries with body size, which in turn covaries with demography (2, 9). There is a long history of studies that examine how body size covaries with population density at equilibrium and whether this covariance matches predictions from metabolic theory (1, 3, 8, 10). For example, because larger species have higher absolute metabolic rates, population density at carrying capacity should covary negatively with body size—and among species, they often do (1, 3, 8, 10). Furthermore, because metabolic rate scales hypoallometrically with body size (4, 11), larger species have lower mass-specific metabolic rates, such that per unit body mass, larger species have lower energy demands. Note that classic metabolic theory focuses on resource use alone—factors such as predation risk, while undoubtedly demographically important (12), do not feature. Consequently, the total biomass of a population at carrying capacity should covary positively with body size (13, 14). For example, because metabolic rate scales with body size at an exponent of around 0.75 in mammals (4), mammal population density should scale with body size at −0.75, and total population biomass should scale with body mass at around 0.25 (5). Meanwhile, the total energy consumption of a population at equilibrium should be mass independent—that is, populations consisting of individuals that differ in their mean body size (but share the same cumulative biomass) should have equivalent energy consumption rates, known as the "energy equivalence rule" (1, 3).

Among-species comparisons of mass and population density have long been used as indirect (albeit compelling) evidence for the negative relationship between energy consumption and density (1, 3, 8, 10). Despite the often-remarkable congruence between predicted and observed relationships between body size and population density among species, these patterns do not directly test the link between metabolic rate and demography. Yet the energy equivalence rule and links between body size and population processes are explicitly mechanistic—body size should affect population processes because of differences in absolute and

Significance

Biology has long-standing rules about how metabolism and demography should covary. These rules connect physiology to ecology but remarkably, these rules have only ever been tested indirectly. Using a model marine invertebrate, we created experimental field populations that varied in metabolic rate but not body size. We show that metabolism qualitatively affects population growth and carrying capacity in ways predicted by theory but that scaling relationships for these parameters, as well as estimates of energy use at carrying capacity, depart from classic predictions. That metabolism affects demography in ways that depart from canonical theory has important implications for predicting how populations may respond to global change and size-selective harvesting.

Author contributions: L.S., H.C., C.R.W., and D.J.M. designed research; L.S. performed research; L.S., H.C., and D.J.M. analyzed data; and L.S., H.C., and D.J.M. wrote the paper.

The authors declare no competing interest.

This article is a PNAS Direct Submission.

[1]L.S. and H.C. contributed equally to this work.

[2]To whom correspondence may be addressed. Email: lukas.schuster02@gmail.com.

This article contains supporting information online at https://www.pnas.org/lookup/suppl/doi:10.1073/pnas.2104942118/-/DCSupplemental.

Published August 20, 2021.

Carrying capacity initially increased with metabolic rate until a local maximum was achieved (when MI-MR was ~ −4) but then declined nonlinearly with any further increase in metabolic rate. While theory predicts a qualitative decline in K with metabolic rate, it is important to note that this decline was shallower than theory predicts (i.e., scaled at an exponent >−1) across much of the parameter space and only approached the predicted scaling exponent of −1 at relatively higher metabolic rates (i.e., values of MI-MR between 7 and 13; Fig. 2*B*).

Finally, the total energy demands of our experimental populations at carrying capacity (ΣE) showed a positive and asymptotic relationship with metabolic rate. Initially, energy demands rose steeply and almost linearly with increases in metabolic rate before beginning to plateau (at values of MI-MR > 0). As such, total energy demands only resembled energy equivalency (i.e., scaled at MR^0) only at very high values of metabolic rate (MI-MR >7 (Fig. 2*C*). Overall then, our results found qualified support for the predicted theoretical relationships between metabolic rate and demography across much of the parameter space explored, but only quantitatively converged with theoretical expectations when population-level metabolic rates were extremely high (MI-MR > 7; Fig. 2).

Discussion

The role of energy and metabolism in shaping ecological patterns and processes has a venerable history of investigation (4, 23–26), yet remains controversial (15, 27)—perhaps because some core principles have only been tested indirectly. We show experimentally that demography is qualitatively affected by metabolic rate in accordance with theory based on among-species patterns. In general, populations with higher metabolic rates showed relatively greater per generation population growth (r) and lower carrying capacities (K). Yet we also found important deviations from theory. Specifically, carrying capacity scaled less steeply than theory predicts (i.e., at an exponent >−1) across much of the parameter space. Consequently, total energy usage at equilibrium was a positively asymptotic function of metabolic rate, rather than being independent of metabolism (i.e., MR^0) as predicted by theory. Importantly, however, we found strong evidence for energy equivalency when metabolic rates were relatively high (Fig. 2). We suggest a critical assumption of classic metabolic theory—the independence of metabolic rate and resource supply—can be violated under field conditions.

Qualitative patterns in key population parameters were congruent with classic metabolic theory (6) across much of the parameter space—populations with higher metabolic rates had relatively lower carrying capacities and higher intrinsic rates of increase. This finding provides direct evidence for a link between metabolism and demography and suggests that such correlations at the interspecific level might also reflect a causal relationship (1, 3). Higher metabolic rates allow for faster biological work, leading to earlier and more reproduction (as reflected by the differences in vital rates among populations; *SI Appendix*, Appendix S2) and subsequent increases in the rate at which populations can grow (6). Similarly, higher metabolism resulted in higher per capita resource demands, such that carrying capacities tended to be lower for higher metabolic rate populations. While more manipulative studies are necessary, at this point it seems that classic metabolic theory can predict population dynamics within species, and that this extends beyond size- and temperature-related trends.

Nevertheless, we observed two (related) departures from theoretical expectations: a concave relationship between metabolic rate and carrying capacity; and a positively asymptotic relationship between metabolic rate and total energy use at equilibrium (Fig. 2). We propose that these departures from classic theory can be reconciled by incorporating perspectives from the increased intake hypothesis (18–20)—that is, by considering that metabolic rate

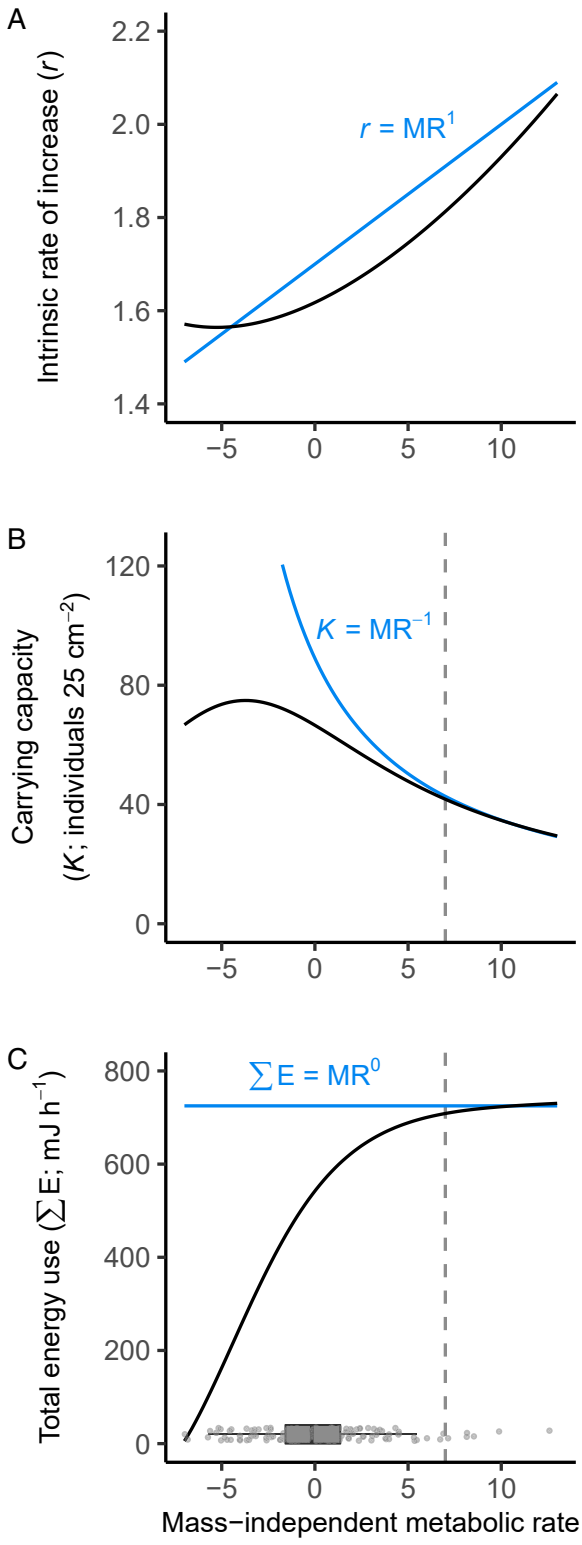

Fig. 2. Relationships between the average metabolic rate (as MI-MR) of our experimental populations and the demographic parameters: (*A*) intrinsic rate of increase (r), (*B*) carrying capacity (K), and (*C*) total energy use at equilibrium (ΣE). Black lines show our empirical estimates; blue lines show classic theoretical predictions. Note that our demographic estimates quantitatively depart from theoretical predictions across most of the parameter space explored, with the exception of estimates of K and ΣE at very high values of metabolic rate (MI-MR > 7; shown by the dotted gray line). Box plot and data points in *C* show the distribution of population-level metabolic phenotypes in our study.

may affect both resource supply and acquisition. Classic metabolic theory explores the special case of resource supply being independent of metabolic rate—thus, any increase in metabolic rate must be perfectly counterbalanced by a decrease in the density of individuals (1, 3, 4). Meanwhile, the increased intake hypothesis holds that resource acquisition positively covaries with metabolism (refer also to ref. 12)—but the implications for population dynamics have not been formally explored.

Intuitively, one might expect that if resource supply increases with metabolic rate, this could offset the increased resource demands associated with populations with higher metabolic rates. As such, K might decline less sharply than at an exponent of -1, leading to an initial increase in total energy use as metabolism increases. This is exactly what we observe—K shows a shallow decline moving from low to higher metabolic rates (in fact, it increases slightly at first), and so, total energy use increases with metabolic rate in this region of parameter space (Fig. 2). Once population-level metabolic rates become sufficiently high, however, any further increase in metabolic rate appears to increase resource demand at a greater rate than resource supply—thus, the total amount of energy being used by the population begins to level off as predicted by theory (1, 3, 6). Although somewhat speculative, this hypothesis seems reasonable—indeed, if we assume a simple (but biologically realistic) asymptotic relationship between metabolic rate and population-level access to resources, we recover almost identical predictions for the relationships between metabolic rate, carrying capacity, and energy use as those that we observe empirically (*SI Appendix*, Appendix S3).

Our hypothesis that metabolism drives resource supply and demand to affect population demography appears most relevant for sessile organisms (plants, fungi, and marine invertebrates)—which comprise much of the life on earth in terms of both biodiversity and abundance. Thus, we suspect such dynamics are likely widespread. In filter-feeding marine invertebrates such as *Bugula*, initial increases in metabolic rate might increase resource supply through more active filter feeding or greater disruption of the benthic boundary layer in higher metabolic rate populations (28, 29). Likewise, the plateauing of energy use as metabolic rates become exceptionally high may occur because the flux of planktonic food in the boundary layer is exhausted, such that further increases in filtering activity yield no further gains in supply (30). Meanwhile, in plants, metabolic rate can affect growth rates and root biomass such that plants with higher metabolic rates may access resources deeper in the soil than plants with lower metabolic rates (and shallower root systems) (31). Under both scenarios, we would expect total resource use to increase with metabolism (at least at first), such that carrying capacities are likely to decline less sharply with metabolic rate than classic theory predicts.

Although less immediately obvious, our results also have applicability to mobile organisms. For example, fish with higher metabolic rates forage more voraciously than fish with lower metabolic rates, potentially accessing more food from their environment (32). While mobile organisms can move and forage in space, allowing them to access new resources, the area from which they draw resources is not infinite. At higher spatial scales, therefore, many of the differences between mobile and sessile consumers collapse. We therefore suspect that in both groups increases in metabolic rate are likely to increase resource access by populations up to a point, but eventually any further increase in metabolic rate (and thus resource demand) will exhaust the local supply, such that carrying capacities should decline.

One important difference between sessile and mobile animals, however, is the potential for metabolic rate, foraging, and predation to interact. In sessile systems (such as ours), predation risk is most likely unrelated to feeding activity or metabolism, but in mobile organisms, higher metabolisms can demand more foraging activity, which also entails greater predation risk (12). Meanwhile, classic metabolic theories focus solely on resource demand and ignore predation, yet these models predict demographic patterns among mobile species, for whom predation is an issue (1, 3, 10). Given that these among-species comparisons often confound body size (which will also affect predation risk), it would be interesting to disentangle whether metabolism affects predation risk independently of body size within mobile species. Regardless, we view our results as strong empirical support for the prescient insight of Houston, McNamara, and Hutchinson (12) that metabolism should affect access to resources. We suggest that the assumption that resource access or supply is insensitive to metabolic rate requires more attention, particularly given its potential to drive covariances between metabolism and demography.

The capacity for metabolic rate to affect resource access is also likely to vary among experimental approaches and could explain variation among previous studies in providing support for theoretical predictions. For example, in contrast to our finding that metabolic rate affects carrying capacity in a curvilinear fashion, Bernhardt, Sunday, and O'Connor (16) showed that carrying capacities scaled with metabolic demands (induced by higher temperatures) in accordance with classic theory (i.e., at MR^{-1}). We suspect differences between our findings and those of Bernhardt, Sunday, and O'Connor (16) arise because in their study, resource supply was sensibly kept constant across temperature treatments—thus, there was no scope for metabolic rate to affect resource supply. In contrast, resource availability could vary naturally in our field experiment—creating the potential for metabolic rate to affect the rate at which populations deplete resources. We thus predict that closed experimental systems—in which resources are regulated—will show different patterns to more open systems in which resources can covary with metabolic rate. We look forward to further tests that directly examine how metabolic rate affects resource access or supply, and the consequences of such dynamics for demography in the field.

Overall, our results support a hybrid of the increased intake hypothesis and energy equivalence, whereby the relative influence of metabolism on resource aquisition and demand, respectively, shifts along a continuum depending on the metabolic rate of the population. This finding contrasts consistent among-species relationships between mass-specific metabolic rate and population density in broad-scale comparisons (1, 3, 4, 8, 10). However, such among-species patterns are not always observed when examined across smaller body size ranges (5, 33, 34). We hypothesize that these apparently contradictory patterns might be reconciled by considering how resource availability varies at different scales and how resource intake covaries with metabolic rate. Energy equivalence may be observed across larger mass ranges, because variation in resource access is small relative to variation in mass-specific metabolic rates among species that differ greatly in size. On the other hand, across smaller mass ranges, variation in resource access might be greater than variation in mass-specific metabolic rates, limiting the ability to detect energy equivalence. Integration of demand- and supply-focused perspectives into metabolic theory has the potential to reconcile the above observations. That carrying capacity is not necessarily inversely proportional to metabolism has potentially far-reaching consequences for predictions of climate change impacts and the management of fisheries (35).

Materials and Methods

Study Species. *B. neritina* Linnaeus, 1758, is a colonial bryozoan common to sessile marine communities worldwide. Growth occurs by the regular budding of zooids (individual subunits) at the colony tips to form symmetrically branched, arborescent colonies (36, 37). Colonies filter-feed by actively extracting phytoplankton from the water column. Importantly, this species shows an approximate twofold variation in metabolic rate that can occur independently of colony size (28, 29, 38–41), and is increasingly used as a model for exploring the ecological consequences of metabolic rate in both laboratory and field settings (28, 39).

Field Collections. We conducted our experiments at the Royal Brighton Yacht Club in Port Phillip Bay, Victoria, Australia, from April to October 2018. We obtained colonies for our manipulations using standard methods (42). Briefly, we collected mature *B. neritina* colonies from the field and induced them to spawn their brooded larvae in the laboratory with light shock after ∼24 h of darkness (43). We settled the released larvae onto roughened A4 acetate sheets (∼200 settlers per sheet), then deployed the settlers into the field by attaching the acetate sheets to the undersides of eight polyvinyl chloride (PVC) backing panels (57 × 57 × 0.6 cm; three acetate sheets per panel) that hung 1 m below the water surface. We retrieved the acetate sheets after 2 wk in the field for use in our experiments. We maintained the acetate sheets bearing experimental colonies in aerated tanks overnight at 19 °C to acclimate them to laboratory conditions.

Measuring Metabolic Rate. Prior to measuring metabolic rate, we cut individual colonies from the acetate sheets (each colony remained attached to an acetate square), and we removed epibionts and debris with a soft paintbrush. We measured rate of oxygen consumption ($\dot{V}O_2$) as a proxy for metabolic rate. Briefly, we measured oxygen consumption with 24-channel sensor dish readers (SDR2, Germany) and 24-chamber glass microplates (750 μl) fitted with nonconsumptive O_2 sensor spots (Loligo Systems, Denmark). The 24-chamber microplates were filled with sterilized, filtered (0.2 μm) seawater: 20 of these chambers received individual *Bugula* colonies; the remaining four chambers received a small square of blank acetate (without a colony attached) to control for microbial oxygen consumption. $\dot{V}O_2$ measurements were taken over 3 h in a dark, constant temperature room at 19 °C. We calculated $\dot{V}O_2$ from the rate of change in oxygen saturation from our traces using local linear regression and the package LoLinR (44, 45). We converted our measures of $\dot{V}O_2$ (milliliters per hour) to metabolic rate (millijoules per hour) with a calorific conversion factor of 20.08 J ml^{-1} O_2 (46). We then measured the body size (as number of zooids) of each colony using a dissecting microscope and converted our measures of absolute metabolic rate to mass-independent values (*SI Appendix*, Appendix S1).

Experimental Design. To test whether metabolic rate alters demographic parameters under field conditions, we created experimental populations that differed in their per capita mass-independent metabolic rates (MI-MRs), as well as population size (density). To create our experimental populations, we glued our *B. neritina* colonies onto PVC plates (55 × 55 × 3 mm) at one of two densities characteristic of those observed in the field (47): a "low-density" treatment (4 individuals per 25 cm^2); and a "high-density" treatment (8 individuals per 25 cm^2). We systematically assigned our *B. neritina* colonies to our experimental populations to generate populations across a continuous range of mean metabolic rates (low density: MI-MR range: −6.98 to 9.88; absolute MR range: 1.15 to 8.95 mJ h^{-1}; high density: MI-MR range: −6.83 to 12.59; absolute MR range: 1.08 to 23.21 mJ h^{-1}; *SI Appendix*, Fig. S1). Importantly, we ensured that within-population variance in metabolic rates were constant across our treatments (low density: mean SD = 0.61; range in SD: 0.06 to 3.48; high density: mean SD = 0.61; range in SD: 0.09 to 3.25). We glued four blank acetate squares (without experimental colonies) onto our low-density plates such that the number of acetate squares were equal among our density treatments.

Field deployment and replication. We deployed our experimental populations (plates) into the field by attaching them to PVC panels (up to 24 plates per panel) as previously described. Due to logistical constraints, we processed a single panel in the laboratory per day, such that the deployment of panels into the field were staggered across a 2-wk period. In total, our experiment consisted of 1,028 *B. neritina* colonies that we deployed across 172 plates (our unit of replication) and eight backing panels.

Measuring Performance. We measured several performance components (vital rates) for all *B. neritina* colonies in our experimental populations every 2 wks across their entire lifetime (April through October 2018).

Survival and growth. At each census, we scored the colonies as alive if they were present on the plates and contained living zooids. Colonies that were absent from the plates or did not contain living zooids were scored as dead and in the latter case were removed from the plates. Values for survival were conditional on survival in the previous census—any colony that had died in a previous census received no value for survival (or any other performance measure) at subsequent census times. We measured growth as the number of times a living colony had branched (bifurcated)—a good proxy for colony biomass (36).

Reproduction and fecundity. We scored reproduction as a binary response variable that indicated whether external reproductive chambers (ovicells) were present on each colony at each census (ovicells present = value of 1; no ovicells = value of 0). Thus, we measured the onset of reproduction. We also measured reproductive output (fecundity) as the number of ovicells present on each colony at each census. Each ovicell houses a single embryo at a time, which is brooded for 1 wk before being released into the plankton as a fully competent, nonfeeding larva. Colonies use ovicells to brood embryos more than once—thus measuring intact ovicells biweekly provides a good indication of lifetime reproductive output (38, 39, 41). Colonies that did not reproduce (received a value of 0 for reproduction) at a given census received no value for fecundity.

Offspring size. We measured the size of second-generation offspring (larvae) produced by our experimental populations after 16 wk in the field (when fecundity was highest). To do this, we spawned each of our experimental populations (plates) in separate containers of seawater as previously described. We collected all larvae released by these populations and fixed them in vials containing 3.5% formalin–seawater solution—these are methods that do not distort larval size (43). We measured the length (micrometers) of ∼50 randomly selected larvae from each population from photographs taken at 100× magnification, and converted larval length to larval mass (micrograms) using an equation that describes this relationship (48).

Modeling Approach. To explore how metabolic rate and population density affect asymptotic population growth rate (λ), we parameterized single-sex, deterministic IPMs with our experimental data (22). While *B. neritina* colonies are simultaneous hermaphrodites, we only consider female performance here.

The model. For each population density, we constructed a size- and age-structured IPM (42, 49):

$$n(z', a, t+1) = \sum_a \int \left[D(z'|z, a, y_m, N_b) M(z, a, y_m, N_b) B(z, a, y_m, N_b) n(z, a, t)\right] dz \quad [1]$$

$$n(z', a+1, t+1) = \int \left[G(z'|z, a, y_m, N_b) S(z, a, y_m, N_b) n(z, a, t)\right] dz. \quad [2]$$

We modeled the continuous trait for size, z, as the number of bifurcations on our colonies, which produced a linear growth curve over the course of our study (*SI Appendix*, Appendix S2 and Fig. S3). Importantly, because *B. neritina* grows via the regular addition of zooids between each bifurcation (colony branch), colony mass scales in direct proportion to bifurcations on a $\log_2$ scale (36). In our models, the first equation deals with new settlers, and the second equation deals with the survival and growth of the colonies. Our models are thus multigenerational—individuals reproduce and recruit into the populations, but we do not model the dispersal of offspring outside their natal environment, nor their planktonic mortality.

$D(z'|z, y_m, a, N_b)$ is the conditional probability density function that describes the distribution of offspring sizes, z', produced by parental colonies of size z at time $t + 1$. a is the experimental age class, y_m is the average mass-independent metabolic rate of our experimental populations, and N_b is the number of *B. neritina* colonies (density) within our experimental populations. For this function, we modeled the Gaussian distribution of offspring sizes (mean = 0.0144 mg ± 0.0017 SD) observed for second-generation offspring, which was independent of parental size and age, as well as the metabolic rate and density of our experimental populations (*SI Appendix*, Appendix S2 and Table S2). $M(z, a, y_m, N_b)$ is a continuous function describing the mean number of offspring produced by an individual with colony size z and of experimental age a given the mean metabolic rate y_m, and initial density N_b of the population. $S(z, a, y_m, N_b)$ and $B(z, a, y_m, N_b)$ are continuous functions that describe the probability of an individual with colony size z and experimental age a at the beginning of the interval surviving and reproducing at the end of the interval, respectively, as a function of population mean metabolic rate and initial population density. $G(z'|z, a, y_b, N_b)$ is the Gaussian probability density function describing transitions from colony size z at time t to colony size z' at time $t + 1$ among survivors as a function of experimental age, metabolic rate, and initial population density. $n(z, t)$ is the distribution of colony sizes at time t such that $N(t) = \int_x^y n(z, t) dz$ is the number of individuals between size z and y. We note that y_m and N_b are experimental factors that we manipulated and are not dynamic in our model. As such, we use our IPMs to estimate asymptotic population growth rates (λ) across the range of population-level metabolic rates and two population densities used in our experimental manipulations. Our IPMs are thus not density-dependent models—that is, our models are not informed by changes in population density throughout the course of the experiment.

Parameterizing the IPMs with our experimental data. To estimate the demographic functions (vital rates) required to parameterize the IPMs, we used generalized linear models on our experimental data (*SI Appendix*, Appendix S2). For numerical solutions of the IPMs, we approximate the integro-difference

ECOLOGY

equation describing the per-time step dynamics with an age- and size-structured matrix, using the midpoint rule for numerical integration (22, 50). The sizes of our *B. neritina* colonies were split into 100 classes that ranged from −2 to 22 bifurcations, and model projections were checked to ensure there was no eviction from the model (51). Colonies rarely grow larger than 22 bifurcations in our study population and never obtained sizes larger than this in our experiment.

As per standard practice, we calculated the asymptotic population growth rate (λ) at equilibrium as the dominant right eigenvectors from our IPMs across our range of metabolic rates. We note that this definition of equilibrium describes when the models had reached a stable population structure and constant population growth rate (52) but does not imply that our experimental populations had reached a constant population size (carrying capacity).

Estimating demographic parameters. In an IPM framework, population parameters such as r and K could be directly estimated from a density-dependent model. Our experiments precluded such an approach for two main reasons: 1) our density manipulations only included two levels, and 2) mortality within our experimental populations was extremely low (*SI Appendix*, Appendix S2), such that densities did not substantially deviate from their initial starting values. To make our IPM density-dependent would thus require extrapolating each vital rate function far beyond our experimental data range (i.e., beyond our two densities), resulting in the substantial propagation of error.

Given the above limitations, we used a two-step approach to estimate relationships between metabolic rate and the demographic parameters of interest. First, as already described, we used our IPMs to integrate the effects of metabolism and initial population density on our experimental measures of performance (vital rates) over time; thus, we obtained reliable estimates of λ across the data range explored. Next, we used these projections of λ from our IPMs to parameterize a Ricker model (53) to obtain estimates of r and K:

$$N_{t+1} = N_t e^{r_0\left(1-\frac{N_t}{K}\right)} \quad [3]$$

$$\frac{N_{t+1}}{N_t} = e^{r_0\left(1-\frac{N_t}{K}\right)}, \quad [4]$$

where r_0 is the intrinsic rate of increase, N_t is population density, K is carrying capacity, and $\lambda = \frac{N_{t+1}}{N_t}$, such that:

$$\lambda = e^{r_o\left(1-\frac{N_t}{K}\right)}. \quad [5]$$

Importantly, a Ricker model provides the best description of density-dependent dynamics in our system (47). Note that although the Ricker model is an unstructured model (53), because we parameterized this model with our estimates of λ from our IPMs, our estimates of both r and K are informed by our vital rate functions and the underlying size- and age-structure in our experimental data.

Rearranging Eq. **5**, we estimated carrying capacity for populations with a given metabolic rate, K_m, by solving simultaneous equations using our estimates of λ_m at low and high density [where $N_{t(low)}$ and $N_{t(high)}$ = 4 and 8 individuals, respectively]:

$$ln\lambda = r_o\left(1-\frac{N_t}{K}\right) \quad [6]$$

$$r_o = \frac{ln\lambda}{1-\frac{N_t}{K}} \quad [7]$$

$$ln\lambda_{m(low)}\left(1-\frac{N_{t(high)}}{K_m}\right) = ln\lambda_{m(high)}\left(1-\frac{N_{t(low)}}{K_m}\right) \quad [8]$$

$$K_m = \frac{-N_{t(low)}ln\lambda_{m(high)} + N_{t(high)}ln\lambda_{m(low)}}{ln\lambda_{m(low)} - ln\lambda_{m(high)}}. \quad [9]$$

Importantly then, our two-step approach allowed us to make inferences within the data range that we explored experimentally, but we acknowledge that an alternative (and more sophisticated) approach would involve manipulations of population-level metabolic rates across a continuous range of population densities (which we did not do here), coupled with explorations of relationships between metabolism and demography via a density-dependent IPM.

From our estimates of K_m, we then solved Eq. **7** to estimate r_{0m}—that is, the intrinsic rate of increase for a population of a given metabolic rate. Finally, we estimated the total energy demands of our experimental populations at equilibrium (ΣE_m) by multiplying our values of K_m by the equation that describes the (average) relationship between mass-independent and absolute metabolic rates (*SI Appendix*, Appendix S1) to project energetic demands in millijoules per hour.

Data Availability. Quantitative data have been deposited in Dryad (https://doi.org/10.5061/dryad.vhhmgqntv) (54).

ACKNOWLEDGMENTS. We are grateful to the Royal Melbourne Yacht Squadron and the Royal Brighton Yacht Club for access to our field sites. We thank Belinda Comerford and Lucy Chapman for field and technical assistance. We also thank Michel Loreau, Martino Malerba, Mariana Álvarez-Noriega, and two anonymous reviewers for insightful comments that greatly improved our manuscript.

1. J. Damuth, Population density and body size in mammals. *Nature* **290**, 699–700 (1981).
2. W. A. Calder, *Size, Function, and Life History* (Harvard University Press, Cambridge, MA, 1984).
3. J. Damuth, Interspecific allometry of population density in mammals and other animals: The independence of body mass and population energy-use. *Biol. J. Linn. Soc. Lond.* **31**, 193–246 (1987).
4. J. H. Brown, J. F. Gillooly, A. P. Allen, V. M. Savage, G. B. West, Toward a metabolic theory of ecology. *Ecology* **85**, 1771–1789 (2004).
5. N. J. Isaac, C. Carbone, B. McGill, "Population and community ecology" in *Metabolic Ecology: A Scaling Approach*, R. M. Sibly, J. Brown, A. Kodric-Brown, Eds. (John Wiley & Sons, Oxford, UK, 2012), pp. 77–85.
6. M. Van Savage, J. F. Gillooly, J. H. Brown, G. B. West, E. L. Charnov, Effects of body size and temperature on population growth. *Am. Nat.* **163**, 429–441 (2004).
7. J. F. Gillooly, E. L. Charnov, G. B. West, V. M. Savage, J. H. Brown, Effects of size and temperature on developmental time. *Nature* **417**, 70–73 (2002).
8. D. M. Perkins *et al.*, Energetic equivalence underpins the size structure of tree and phytoplankton communities. *Nat. Commun.* **10**, 255 (2019).
9. R. H. Peters, *The Ecological Implications of Body Size* (Cambridge University Press, New York, 1986), vol. 2.
10. I. A. Hatton *et al.*, The predator-prey power law: Biomass scaling across terrestrial and aquatic biomes. *Science* **349**, aac6284 (2015).
11. M. Kleiber, Body size and metabolism. *Hilgardia* **6**, 315–353 (1932).
12. A. I. Houston, J. M. McNamara, J. M. Hutchinson, General results concerning the trade-off between gaining energy and avoiding predation. *Philos. Trans. R. Soc. B* **341**, 375–397 (1993).
13. B. A. Maurer, J. H. Brown, Distribution of energy use and biomass among species of North American terrestrial birds. *Ecology* **69**, 1923–1932 (1988).
14. T. M. Blackburn, K. J. Gaston, Body size and density: The limits to biomass and energy use. *Oikos* **69**, 336–339 (1994).
15. D. Tilman *et al.*, Does metabolic theory apply to community ecology? It's a matter of scale. *Ecology* **85**, 1797–1799 (2004).
16. J. R. Bernhardt, J. M. Sunday, M. I. O'Connor, Metabolic theory and the temperature-size rule explain the temperature dependence of population carrying capacity. *Am. Nat.* **192**, 687–697 (2018).
17. D. C. Reuman, R. D. Holt, G. Yvon-Durocher, A metabolic perspective on competition and body size reductions with warming. *J. Anim. Ecol.* **83**, 59–69 (2014).
18. P. A. Biro, J. A. Stamps, Do consistent individual differences in metabolic rate promote consistent individual differences in behavior? *Trends Ecol. Evol.* **25**, 653–659 (2010).
19. M. A. Chappell, T. Garland Jr, G. F. Robertson, W. Saltzman, Relationships among running performance, aerobic physiology and organ mass in male *Mongolian gerbils*. *J. Exp. Biol.* **210**, 4179–4197 (2007).
20. B. K. McNab, Food habits, energetics, and the population biology of mammals. *Am. Nat.* **116**, 106–124 (1980).
21. S. Nee, A. F. Read, J. J. Greenwood, P. H. Harvey, The relationship between abundance and body size in British birds. *Nature* **351**, 312 (1991).
22. M. R. Easterling, S. P. Ellner, P. M. Dixon, Size-specific sensitivity: Applying a new structured population model. *Ecology* **81**, 694–708 (2000).
23. R. L. Lindeman, The trophic-dynamic aspect of ecology. *Ecology* **23**, 399–417 (1942).
24. H. T. Odum, Efficiencies, size of organisms, and community structure. *Ecology* **37**, 592–597 (1956).
25. D. M. Gates, Energy, plants, and ecology. *Ecology* **46**, 1–13 (1965).
26. M. Loreau, *From Populations to Ecosystems: Theoretical Foundations for a New Ecological Synthesis* (Princeton University Press, Princeton, NJ, 2010).
27. M. P. O'Connor *et al.*, Reconsidering the mechanistic basis of the metabolic theory of ecology. *Oikos* **116**, 1058–1072 (2007).
28. G. Ghedini, C. R. White, D. J. Marshall, Does energy flux predict density-dependence? An empirical field test. *Ecology* **98**, 3116–3126 (2017).
29. M. K. Lovass, D. J. Marshall, G. Ghedini, Conspecific chemical cues drive density-dependent metabolic suppression independently of resource intake. *J. Exp. Biol.* **223**, jeb224824 (2020).
30. M. E. Lagos, C. R. White, D. J. Marshall, Do invasive species live faster? Mass-specific metabolic rate depends on growth form and invasion status. *Funct. Ecol.* **31**, 2080–2086 (2017).

31. L. D. Hansen *et al*., The relation between plant growth and respiration: A thermodynamic model. *Planta* **194**, 77–85 (1994).
32. S. K. Auer *et al*., Metabolic rate interacts with resource availability to determine individual variation in microhabitat use in the wild. *Am. Nat.* **196**, 132–144 (2020).
33. N. J. B. Isaac, D. Storch, C. Carbone, J. Kerr, The paradox of energy equivalence. *Glob. Ecol. Biogeogr.* **22**, 1–5 (2013).
34. M. E. Malerba, D. J. Marshall, Size-abundance rules? Evolution changes scaling relationships between size, metabolism and demography. *Ecol. Lett.* **22**, 1407–1416 (2019).
35. J. L. Blanchard, R. F. Heneghan, J. D. Everett, R. Trebilco, A. J. Richardson, From bacteria to whales: using functional size spectra to model marine ecosystems. *Trends Ecol. Evol.* **32**, 174–186 (2017).
36. M. J. Keough, H. Chernoff, Dispersal and population variation in the bryozoan *Bugula neritina*. *Ecology* **68**, 199–210 (1987).
37. M. J. Keough, Variation in growth rate and reproduction of the bryozoan *Bugula neritina*. *Biol. Bull.* **177**, 277–286 (1989).
38. A. K. Pettersen, C. R. White, D. J. Marshall, Metabolic rate covaries with fitness and the pace of the life history in the field. *Proc. Biol. Sci.* **283**, 20160323 (2016).
39. A. K. Pettersen, M. D. Hall, C. R. White, D. J. Marshall, Metabolic rate, context-dependent selection, and the competition-colonization trade-off. *Evol. Lett.* **4**, 333–344 (2020).
40. L. Schuster, C. R. White, D. J. Marshall, Influence of food, body size, and fragmentation on metabolic rate in a sessile marine invertebrate. *Invertebr. Biol.* **138**, 55–66 (2019).
41. L. Schuster, C. R. White, D. J. Marshall, Plastic but not adaptive: Habitat-driven differences in metabolic rate despite no differences in selection between habitats. *Oikos* **130**, 931–942 (2021).
42. H. Cameron, T. Coulson, D. J. Marshall, Size and density mediate transitions between competition and facilitation. *Ecol. Lett.* **22**, 1879–1888 (2019).
43. D. J. Marshall, T. F. Bolton, M. J. Keough, Offspring size affects the post-metamorphic performance of a colonial marine invertebrate. *Ecology* **84**, 3131–3137 (2003).
44. C. R. White, M. R. Kearney, P. G. Matthews, S. A. Kooijman, D. J. Marshall, A manipulative test of competing theories for metabolic scaling. *Am. Nat.* **178**, 746–754 (2011).
45. C. Olito, C. R. White, D. J. Marshall, D. R. Barneche, Estimating monotonic rates from biological data using local linear regression. *J. Exp. Biol.* **220**, 759–764 (2017).
46. D. Crisp, "Energy flow measurements" in*Methods for the Study of Marine Benthos*, N. A. Holme, A. D. McIntyre, Eds. (Blackwell, Oxford, UK, 1971), pp. 197–279.
47. S. P. Hart, D. J. Marshall, Environmental stress, facilitation, competition, and coexistence. *Ecology* **94**, 2719–2731 (2013).
48. A. K. Pettersen, C. R. White, D. J. Marshall, Why does offspring size affect performance? Integrating metabolic scaling with life-history theory. *Proc. Biol. Sci.* **282**, 20151946 (2015).
49. T. Coulson, S. Tuljapurkar, D. Z. Childs, Using evolutionary demography to link life history theory, quantitative genetics and population ecology. *J. Anim. Ecol.* **79**, 1226–1240 (2010).
50. S. P. Ellner, D. Z. Childs, M. Rees, *Data-Driven Modelling of Structured Populations. A Practical Guide to the Integral Projection Model* (Springer, Cham, 2016).
51. J. L. Williams, T. E. Miller, S. P. Ellner, Avoiding unintentional eviction from integral projection models. *Ecology* **93**, 2008–2014 (2012).
52. H. Caswell, *Matrix Population Models: Construction, Analysis and Interpretation* (Oxford University Press, Inc., Oxford, UK, ed. 2, 2006).
53. W. E. Ricker, Stock and recruitment. *J. Fish. Res. Board Can.* **11**, 559–623 (1954).
54. L. Schuster, H. Cameron, C. White, D. Marshall, Data from: Metabolism drives demography in an experimental field test. *Dryad*. https://datadryad.org/stash/dataset/doi:10.5061/dryad.vhhmgqntv. Deposited 5 August 2021.